Gail E. Marlow
B. Montgomery Pettitt
Department of Chemistry, University of Houston, Houston, TX 77204-5641

Simulations of the Bis-Penicillamine Enkephalin in Sodium Chloride Solution: A Parameter Study

Abstract: *A simulation study of DPDPE in sodium chloride solution has been performed and compared with previous simulations using a different interaction potential for the ions. Both global thermodynamics as well as a characterization of association to DPDPE have been calculated. We show that the parameters used for the ions have a profound effect on the association to the peptide in 1*M *NaCl. The observed differences suggest that individual associations in these and previous simulations are sensitive to parameters.* © 2001 John Wiley & Sons, Inc. Biopolymers (Pept Sci) 60: 134–152, 2001

Keywords: *bis-penicillamine enkephalin; sodium chloride; thermodynamics*

INTRODUCTION

Both the physical and chemical properties of proteins and peptides in solution are exquisitely sensitive to the solution environment. The addition of ions can strongly alter the thermodynamic and structural properties of peptides in solution.[1–3] Even very small changes, on the order of 0.1*M*, in the ionic strength of the solution can lead to dramatic changes in the solubility and stability of the protein or peptide solute. This is experimentally evident in the ability of ionic compounds to alter the solubility of peptide and protein solutes in aqueous solution.[3–5] An increase in the solubility of the solute with increasing salt concentration is called the salting in effect, and a decrease in the solubility of a solute with increasing salt concentration is called salting out. The latter leads to the formation of a precipitate. Alteration of protein stability leading to denaturation of the native conformation by changes in salt activity has also been studied extensively by experiment.[1,2,6,7] Changes in conformational stability and solubility of peptides and proteins in solution are clearly coupled and interdependent in a number of systems.[8]

While understanding the underlying causes of these phenomena is of fundamental interest to the study of the physical chemistry of solutions of peptides and proteins in aqueous electrolytes, numerous important potential applications exist.[9,10] For example, it is known that peptides with lengths of less than 20 amino acid residues are hormones and mediators for various biological processes. The thermally accessible conformations of these molecules and the distribution of these conformations are central to understanding their physiological activity. Both the conformations and their distribution are dependent on the concentration and identity of ions present in the solution, and understanding the nature of these dependencies is helpful in terms of medicinal chemistry. In recent years, molecular biological and biotechnical techniques have grown to make the modification of the structure of proteins a realistic experimental endeavor. In general, drug activity is known to be sensitive to pH and environment polarity. Improved knowledge of the microscopic basis for these observations may enhance understanding of the mechanism of drug action and may be useful in the design of new

Biopolymers (Peptide Science), Vol. 60, 134–152 (2001)

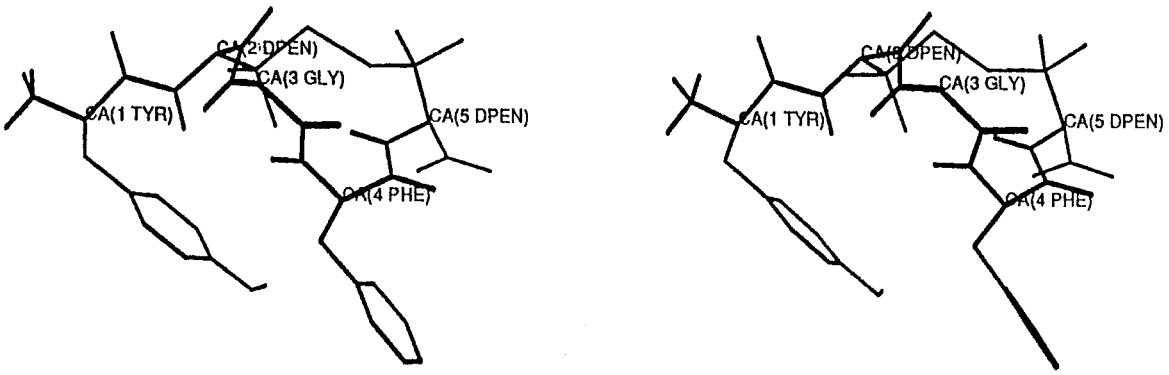

FIGURE 1 Stereoview of the initial conformation of DPDPE (taken from Ref. 41).

pharmaceuticals with improved selectivity and/or potency. With physiological salt concentration in the 0.15*M* range and with a wide range of ion types present (Na^+, K^+, Cl^-, HCO_3^-, etc.), the effects of salt on the action and potency of potential pharmaceuticals can not be ignored.

In particular, the conformation of peptides is known to be sensitive to the details of the solution environment.[1–3,8,11–19] The shapes available, bulk solubility, and thermodynamics of binding are strongly affected by relatively small changes in the salt activities of the solution. Many peptides, especially short ones (less than 10 residues in length), often do not adopt a single conformation in solution as supported by nuclear Overhauser effect (NOE) measurements in aqueous solution.[20] It is well known that differences in cation or anion charges, as well as their relative sizes and polarizability, have important consequences on the solvation of ions by water and the subsequent interaction of these solvated ions with biomolecules.[12,21–23] The effects of these differences on peptides and proteins are expressed in the lyotropic or Hofmeister series.[13,24,25] The effects of ions are thus ordered according to their ability to denature a protein or to increase or decrease the solubility of a peptide in solution.

Hofmeister effects have been studied directly and indirectly by experimental, theoretical, and computational methods. While many trends have been observed, little atomic detail about the processes underlying the observed effects is known. In addition to being fundamentally relevant to the study of the behavior of peptides and proteins in solution, this level of understanding can potentially provide clues about which modifications to molecular structure can produce desired biological or pharmaceutical activity. One of the primary benefits of the computational method of molecular dynamics simulation is that it provides the degree of atomic detail necessary to study the factors underlying the Hofmeister series on a microscopic level. It also presents the opportunity to observe time correlations between the behavior and properties of ions in solution and the subsequent interactions between ions and a peptide or protein solute, information that is difficult to extract from experimental data alone.

The inclusion of salt in molecular dynamics simulations of biological systems presents certain difficulties.[26,27] Even so, the ability of molecular dynamics to provide atomic level detail makes it an attractive method for use in the investigation of the microscopic nature of the Hofmeister series. Some of the first studies including ions and explicit water with a biological molecule involved the simulation of proteins in their observed crystalline environment.[28,29] Although some investigation of the interaction between ions and the protein was conducted, ions were present primarily to maintain electroneutrality. The main focus of these studies was to compare structural data obtained from molecular dynamics simulation with those obtained from x-ray data. We have used molecular dynamics to look directly at the effects of salt on the properties and characteristics of a peptide in aqueous solution, and therefore indirectly at the origins of the Hofmeister series. The inclusion of ions in molecular dynamics simulations requires the choice of parameters for those ions, and several parameter sets are available. Part of the initial motivation for the current work was to make a comparison between simulations that employed different parameters for the ions in a peptide–water environment.

Hofmeister effects have been examined previously in this lab through the simulation of the zwitterionic bis(penicillamine) enkephalin derivative of sequence Tyr–[D]Pen–Gly–Phe–[D]Pen known as DPDPE, shown in Figure 1. We have used molecular dynamics to study DPDPE in aqueous sodium chloride[30,31] and in aqueous sodium acetate.[32] DPDPE was designed

using [D]penicillamine residues, isopropylcysteine derivatives with sulfur-containing side chains, to form a constrained macrocyclic ring structure through the formation of a disulfide bond between the residues. DPDPE is a pharmacologically interesting molecule, developed as a synthetic neurotransmitter to map the structure of the δ-opioid receptor.[33–38] Studies demonstrated that DPDPE is the most specific and one of the most potent neurotransmitters for the δ-opioid receptor ever found.[39] Because its conformational freedom is limited by the disulfide linkage forming the macrocycle,[40,41] the primary sites of flexibility on DPDPE reside with the aromatic side chains of tyrosine and phenylalanine. These groups are believed to be associated with the pharmacophore of δ-opioid receptor neurotransmitters, and their conformation is thought to be largely determined upon binding to the receptor.[20,38,39] These properties make DPDPE an appealing choice from a computational aspect as well as a pharmacological one. DPDPE is large enough to exhibit limited flexibility in structure, yet small enough to be practical to adequately sample the phase space associated with the system computationally. In addition, the conformational degrees of freedom are limited due to the presence of the disulfide linkage and the steric hindrance provided by the geminal methyl groups on the C_β atoms of the [D]penicillamine residues that constrain the macrocycle, further reducing the conformational sampling required. DPDPE has been studied by NMR,[20,42,43] x-ray crystallography,[44] molecular modeling and mechanics,[20,40,41,43,45–49] and molecular dynamics.[41,50,51]

The motivation for the current study was threefold. First, the previous study of DPDPE in sodium chloride involved two simulations of 200 ps each. Improvements in computational speed have increased the feasibility of longer simulation times, which improve sampling, thereby increasing confidence in results obtained and, hopefully, agreement with experiment. Second, we wanted to reexamine the system using the optimized potential surface (OPLS) parameter set,[52] which was parameterized to reproduce structural data on fluids and was optimized for use in the computer simulation of liquids. This would, presumably, provide a more realistic description of the effect sodium chloride exerts on a peptide solute and would allow comparison to other simulations underway or planned in this lab that employ OPLS nonbonded parameters. Third, extension of our previous 250 ps simulation of DPDPE in water[41] would provide an improved baseline, or control, for comparison of DPDPE in solution of OPLS sodium chloride. Results from this simulation are included only as warranted for comparison to the current sodium chloride study.

Our previous simulation of DPDPE in aqueous solution of sodium chloride[30,31] employed a combination of parameters. The peptide and peptide–water interactions were modeled using CHARMm[53] bonded and OPLS[52] nonbonded interactions. Only polar hydrogens were included. Ion–water parameters were taken from a previous study.[54] These parameters were obtained through parameterization of molten salts[55,56] and so comparison with the OPLS set parameterized for aqueous solution is interesting for a number of reasons.

In the next section, we present the methodology and details of the current simulation. The third section contains the results and discussion of the effect of added sodium chloride on the properties of DPDPE in water, and a comparison between the simulations of DPDPE in aqueous solution of the ions in the two parameter sets. Potential implications for peptides in solution and the molecular dynamics simulation of these systems will be discussed.

METHOD

A molecular dynamics simulation of DPDPE was performed in an aqueous solution of approximately 1.0*M* sodium chloride. The system contained DPDPE, 411 water molecules, 9 sodium ions, and 9 chloride ions in a cubic box of length 24.00 Å. The volume of the simulation box was reduced in accordance with the reduced partial molar volume of the ions. To generate an initial configuration, DPDPE was placed into a previously equilibrated box of water. Any waters within 2.3 Å of the peptide were removed. The initial conformation of DPDPE corresponded to that obtained from a previous molecular dynamics study.[40] Ions were inserted by randomly replacing water molecules. The system was then relaxed with 100 steps of steepest descent minimization.

The peptide and ion force field incorporated OPLS[52,57] nonbonded parameters in combination with CHARMm[53] bonded parameters. A flexible SPC water model[58] was used for the solvent with a correspondingly conservative time step of 0.5 fs and the velocity Verlet algorithm for the integration of the equations of motion. All electrostatic interactions were calculated using the Ewald procedure,[59,60] thereby avoiding the problems associated with the use of electrostatic cutoffs.[30,31]

Initial velocities were assigned from a Maxwell–Boltzmann distribution at 300 K. The system was allowed to evolve for 30 ps with intermittent reassignment of velocities. A further 50 ps of equilibration were then performed in the microcanonical (NVE) ensemble. Finally, 1200 ps of production were performed, making a total of 1280 ps.

Table I Average Energies

Energy	Avg. (kJ/mol)
Total PE	−24479
Total KE	4985
Total T	306
Solute PE	343
Solvent PE	−13230
Solute—Solv PE	−796
Solute—Ion PE	−578
Solvent—Ion PE	−7192
Ion-Ion PE	−3062
Na^+—Solute PE	−479
Na^+—Solvent PE	−3815
Cl^-—Solute PE	−99
Cl^-—Solvent PE	−3378
Na^+—Na^+ PE	11405
Na^+—Cl^- PE	−25825
Cl^-—Cl^- PE	11357

The trajectory of the original DPDPE-water simulation,[41] which contained 429 water molecules in a 24.17 Å box, was extended to a length of 1 ns by using the final system configuration in that simulation for the initial configuration in the current DPDPE–water simulation.

The previous σ and ϵ Lennard–Jones parameters for sodium and chloride ions were extracted from sodium–water and chloride-water parameters from a non-Lennard–Jones force field and used to calculate interactions between DPDPE and the ions. The ion–ion interactions were modeled with a Born–Huggins–Mayer potential with parameters taken from Ref. 54. This resulted in values of $\sigma_{Na} = 0.222$ nm, $\sigma_{Cl} = 0.388$, $\epsilon_{Na} = 0.6305$ kJ/mol, and $\epsilon_{Cl} = 4.5551$ kJ/mol. These values are considerably different from the OPLS set. For the OPLS set, the chloride ion in particular is nearly $\frac{3}{4}$ Å larger. This has a profound effect on aqueous solubility of the salt alone[8] and the effect on peptide–salt correlations might be expected to be significant as well.

RESULTS AND DISCUSSION

The trajectory performed here was analyzed in terms of both thermodynamic and time-dependent properties. In addition, extensive comparisons with previously published simulations from this laboratory have been performed.

Thermodynamic Averages

Averages for thermodynamic properties obtained from the simulation are presented in Table I. In order to increase computational speed, a change in the implementation of the Ewald sum was made since the previous simulation of DPDPE in aqueous sodium chloride. This change allowed for the decomposition of the potential energy into additional terms in the current simulation. This, combined with the use of a different force field for the ions, makes direct comparison to the thermodynamic averages from the previous simulation more difficult; however, comparisons within the simulation and to the DPDPE–water simulation are straightforward.

The potential energy between DPDPE and water was negative, indicating a favorable interaction; however, it was less negative than in the simulation of the peptide in aqueous solution where an average of −1189 kJ/mol was obtained. This was due primarily to the presence of the ions, which provided an additional component to the solution environment around the peptide. The potential energy between solvent molecules was also less favorable than it was in the peptide–water simulation where an average of −17253 kJ/mol was obtained. The value of −13230 kJ/mol, found for the solvent in the current simulation, still indicates a strong favorable interaction, but less so. This is to be expected because of the presence of ions in the solution. In order for water to solvate the ions, hydrogen-bonding interactions between water molecules must be disrupted. In addition, groups on the peptide must be desolvated in order for a direct association with an ion to occur. Both the solvent's interactions with the peptide and with itself were therefore reduced (made less negative). The overall interaction of ions with the peptide was favorable, as was the overall interaction between ions and solvent, more than compensating for the observed decreases. It should also be noted that the ion–ion potential energy had a sizable negative value of −3063 kJ/mol. In this simulation, the interactions of sodium and chloride ions were decomposed into components of potential energy between each ion type with the peptide, water, its counterion, and like ions. Potential energies between like ions were positive, as would be expected due to repulsion of like charges. All of the other averages involving the potential energies of ions, however, were negative and therefore, favorable. The addition of ions seems to have destabilized the interactions within DPDPE; however, the solute potential energy, which was only slightly positive in the case of pure water, increased in size.

Time histories for potential energies describing the interaction of the peptide with its solution environment are displayed in Figure 2. A general increase in the value of the potential energy of DPDPE with water occurred gradually over the simulated period. This is consistent with a gradual desolvation of the peptide as interactions between the peptide and water were replaced by interactions with ions. A seemingly

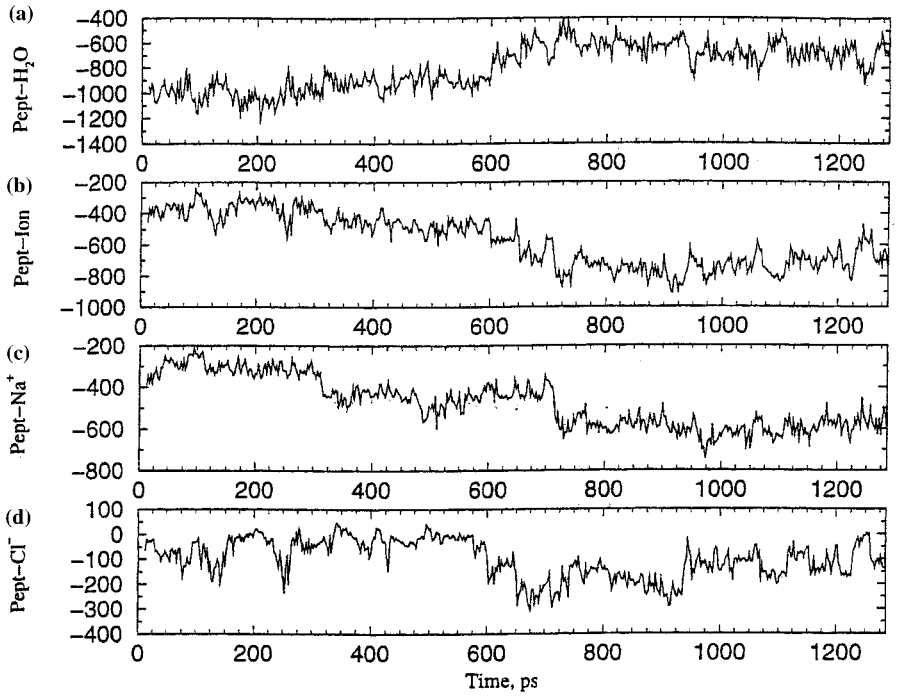

FIGURE 2 Energy time histories for the DPDPE in NaCl simulation. (a) Peptide—H_2O, (b) peptide–ion, (c) peptide–Na^+, and (d) peptide–Cl^-.

concomitant decrease in the value of the peptide–ion potential energy can be seen. This energy was essentially a mirror image of the peptide–solvent potential energy indicating a gradual desolvation of DPDPE as the peptide exchanged interactions with water for interactions with ions. The peptide–ion time histories demonstrate that contributions to the peptide–ion potential energy came from both the cation and the anion. While the magnitude of the interaction with the peptide was different, both sodium and chloride experienced a favorable interaction with DPDPE and, therefore, contributed to the overall strength of the interaction between ions and the solute. In the simulation of DPDPE in aqueous solution of BHM ions, a similar desolvation of the peptide was observed over the course of the simulation in exchange for an increasingly favorable DPDPE–ion potential energy. In that simulation, however, the favorable contributions came only from interaction of chloride ions with the peptide and not from both ionic species, as observed here.

Solvation and Solution Properties

The potential energies describing the interaction of sodium and chloride ions with DPDPE reflect binding of ions to the peptide, both in terms of direct contact and through solvent-mediated interactions. A thorough analysis of ion binding events has been performed. Binding of each of the nine sodium ions to the carboxylate terminus and to each of the four carbonyl groups of the peptide backbone was investigated by plotting the distance between these groups as a function of time. Similarly, the distance between each of the nine chloride ions and the ammonium terminus and each of the N—H groups of the peptide backbone was plotted over the simulation period. The results are summarized in Table II with listings according to the group on the peptide. The ion investigated, number of binding events to that group, and

Table II Ion Binding to the Peptide

Peptide Group	Species Bound	No. Events	Duration (ps)
NT	Cl^-	3	335, 160, 45
N_{17}—H (dpen 1)	—	0	—
N_{26}—H (gly)	Cl^-	3	30, 160, 2
N_{31}—H (phe)	Cl^-	1	10
N_{43}—H (dpen2)	—	0	—
CT	Na^+	2	570, 1285
$C{=}O_{16}$ (tyr)		0	—
$C{=}O_{25}$ (dpen1)	Na^+	1	185
$C{=}O_{30}$ (gly)	Na^+	2	60
$C{=}O_{42}$ (phe)	Na^+	4	765, 130, 40, 5

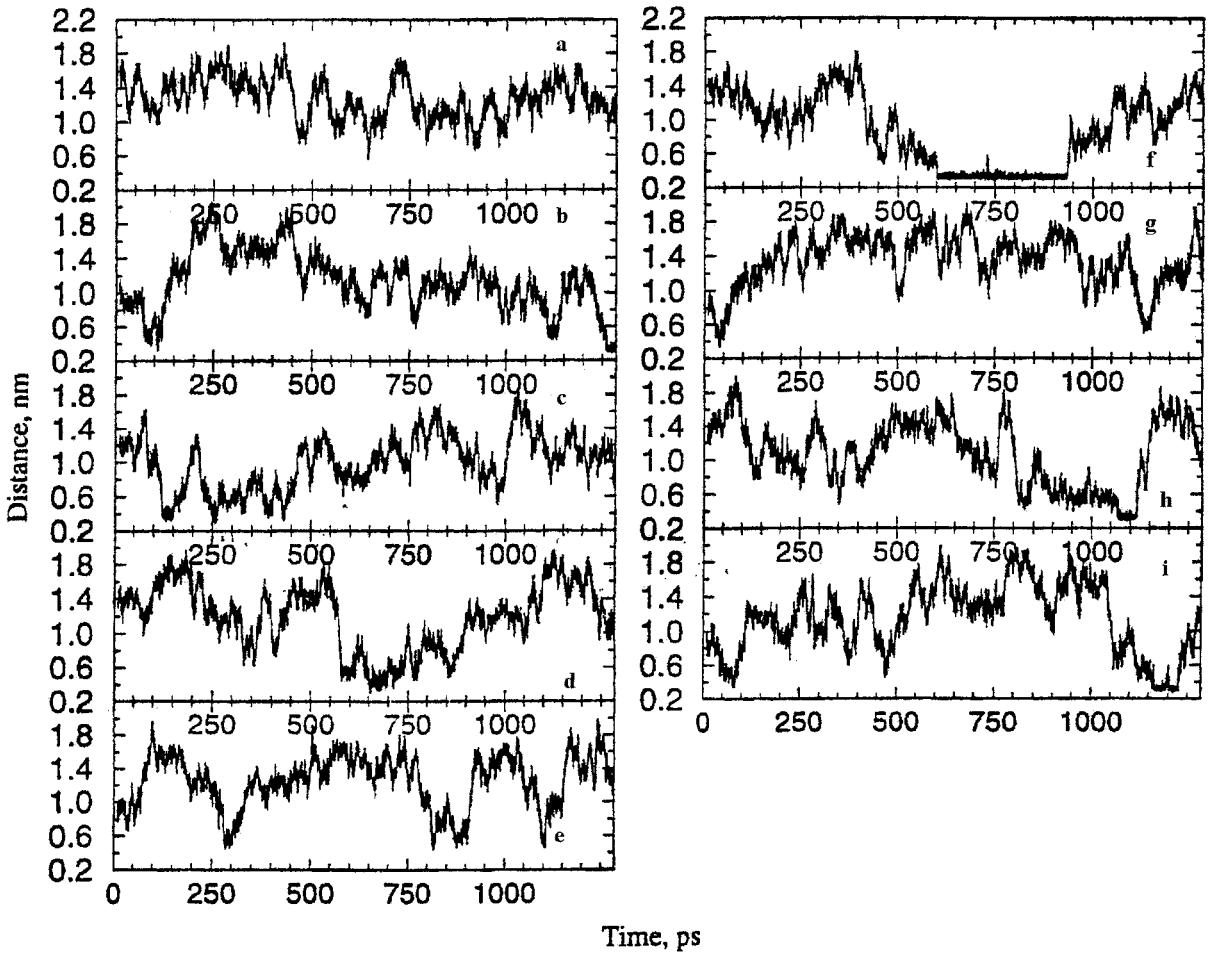

FIGURE 3 Distance time histories of N-terminus to all nine Cl^- ions for the DPDPE in NaCl simulation. (a) NT-Cl^- 1, (b) NT–Cl^- 2, (c) NT–Cl^- 3, (d) NT–Cl^- 4, (e) NT–Cl^- 5, (f) NT–Cl^- 6, (g) NT–Cl^- 7, (h) NT–Cl^- 8, and (i) NT–Cl^- 9.

duration of each event is noted. Both terminal groups experienced binding and several instances of temporary ion binding to the peptide backbone were observed. A variety of durations of binding was observed for each group involved in binding. In some instances, the same ion bound to the peptide repeatedly, sometimes binding to the same group and sometimes binding to different groups.

This is in marked contrast to the binding observed in the simulation with Born–Huggins–Mayer (BHM) sodium chloride. There, all nine chloride ions bound to the peptide, most within the first 50 ps of the trajectory, and none were exchanged over the duration of the trajectory. It should the noted that the entire trajectory was only 200 ps long. Some of the binding events observed in the current simulation for a few of the chloride ions were nearly that long, or longer, suggesting that some of the BHM chlorides could have been exchanged if the simulation had been extended. On the other hand, the differences in solubilities between the two force fields may have prevented this, regardless of the length of the trajectory. This will be discussed further in the last section.

Time histories for distances between the peptide and ions are shown in Figures 3–5. Figure 3 displays the time histories of each of the nine chloride ions to the nitrogen of the N-terminus. Six of the nine ions did not interact directly with the terminal group; three of the nine did. The chloride ion shown in Figure 3f was bound for the longest period of any chloride ion, 335 ps. The other two ions bound for much shorter periods of time. The ion pictured in Figure 3i began to diffuse toward the N-terminus at about 1100 ps, binding at 1170 ps. It remained bound for approximately 160 ps and then diffused away. The shortest binding event to the terminal group occurred between 1070 ps and 1115 ps, and is shown in Figure 3h. This same

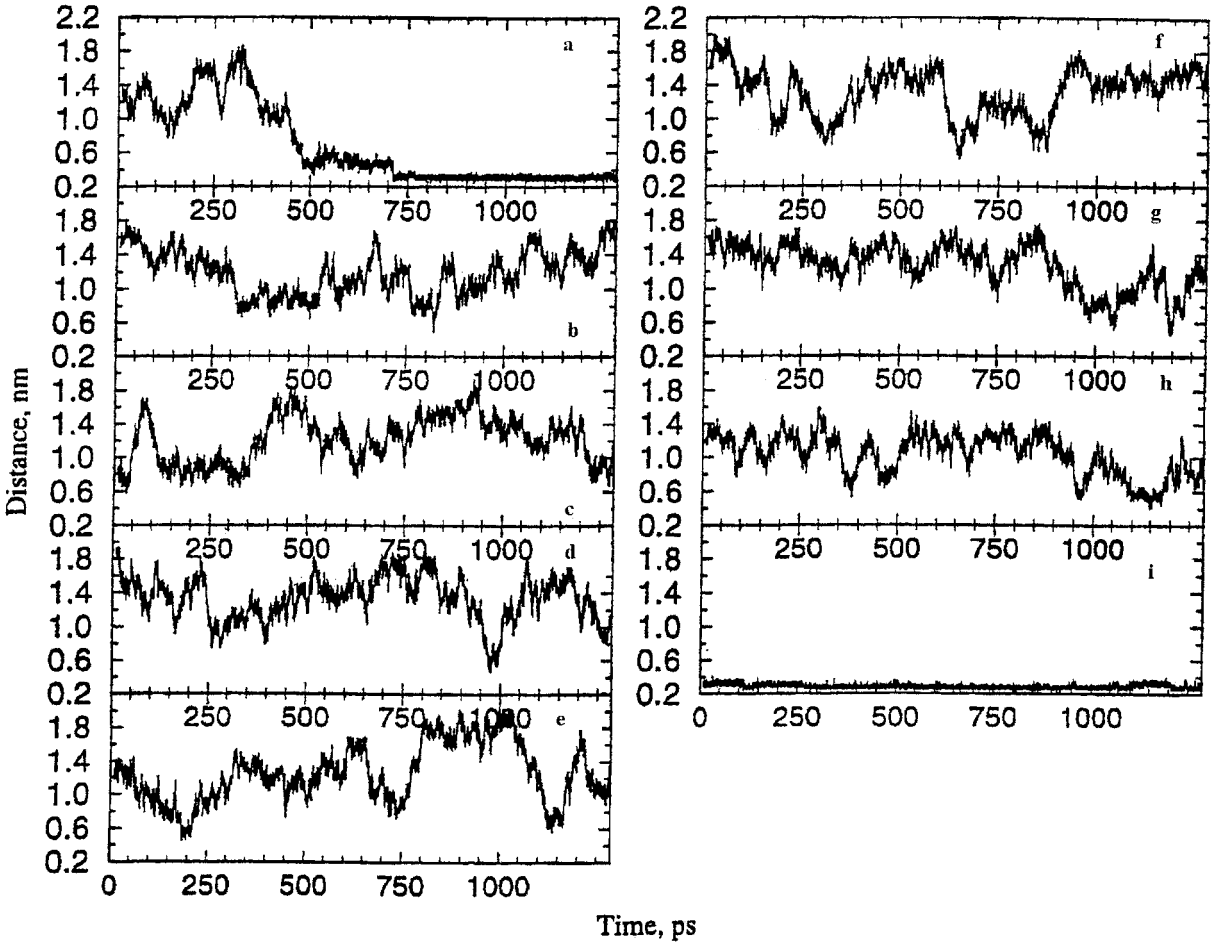

FIGURE 4 Distance time histories of C-terminus to all nine Na^+ ions for the DPDPE in NaCl simulation. (a) CT–Na^+ 1, (b) CT–Na^+ 2, (c) CT–Na^+ 3, (d) CT–Na^+ 4, (e) CT–Na^+ 5, (f) CT–Na^+ 6, (g) CT–Na^+ 7, (h) CT–Na^+ 8, and (i) CT–Na^+ 9.

chloride ion had been bound to the peptide backbone, to the N—H group on glycine, for 160 ps (Figure 5h). It diffused away from the glycine at 1060 ps and bound to the N-terminus at 1070 ps.

Association of sodium ions appeared to be longer lived than chloride ion association. Time histories for the distance between the carbon atom of the C-terminus and all nine sodium ions are shown in Figure 4. Longer durations of association were observed. The sodium ion in Figure 4a was bound to the C-terminus for nearly half of the simulated period. The ion seen in Figure 4i was near the C-terminus in the initial configuration. This ion approached the terminal group during the equilibration period, was bound to it by the start of production, and was not exchanged during the simulation. This is notably different from the N-terminus, where every chloride ion bound was exchanged over the period of the simulation. In the simulation of DPDPE in BHM ions, sodium ions moved away from the peptide and no binding was observed.

Both sodium and chloride ions were found on occasion to associate with multiple groups on the peptide simultaneously. One chloride ion bound to N_{26}—H of glycine at 715 ps. At 735 ps this ion was briefly (<10 ps) in association with N_{31}—H of phenylalanine as well. This interaction did not appear to be particularly favorable, as the ion diffused away from both groups at 745 ps. One of the sodium ions bound to the carbonyl of phenylalanine ($C{=}O_{42}$) at 485 ps as seen in Figure 5d. After about 50 ps, at 535 ps, this same ion also bound to the carbonyl of glycine ($C{=}O_{30}$) for about 25 ps (Figure 5b). The interaction between the sodium ion and glycine was short-lived, but the ion remained bound to the phenylalanine carbonyl. At 715 ps, this same ion began an interaction with the C-terminus that persisted for the remainder of the simulation. For about 30 ps at the end of the

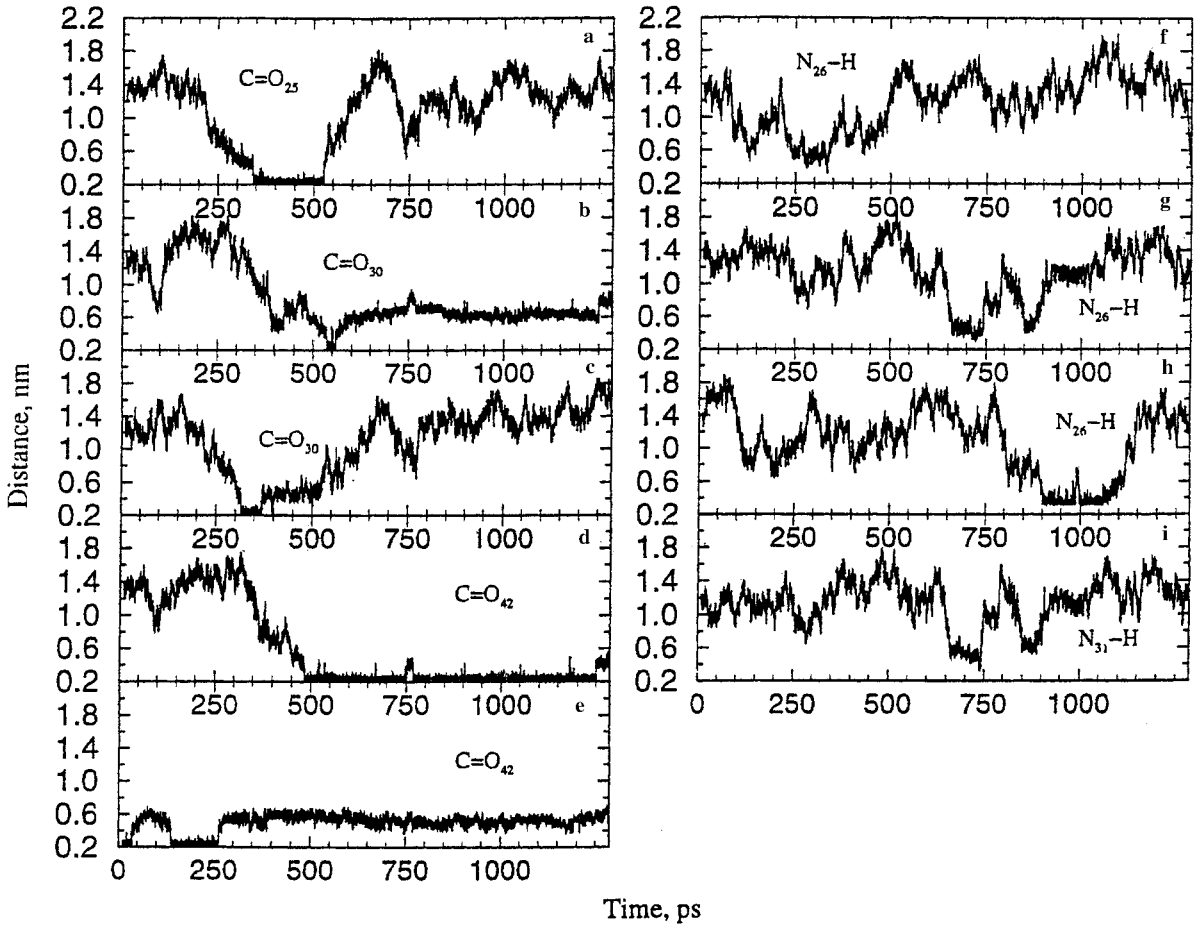

FIGURE 5 Distance time histories of backbone C=O groups to Na^+ and backbone N—H groups to Cl^- for the DPDPE in NaCl simulation. (a) $C=O_{25}$, (b) $C=O_{30}$, (c) $C=O_{30}$, (d) $C=O_{42}$, (e) $C=O_{42}$, (f) N_{26}–H, (g) N_{26}–H, (h) N_{26}–H, and (i) N_{31}—H.

simulation, this ion released its hold on the phenylalanine carbonyl and interacted only with the C-terminus. In the last 5 ps, the sodium ion resumed its joint interaction with both the terminal group and the carbonyl. Recall that one of the sodium ions was bound to the C-terminus for the length of the simulation, so association of any additional sodium ion indicates two ions bound simultaneously to the terminal group.

This behavior was also observed for other sodium ions. Another ion, seen in Figure 5c, bound to the carbonyl of glycine ($C=O_{30}$) at 310 ps. After about 30 ps, it also bound to the carbonyl of the first [D]penicillamine residue ($C=O_{25}$) as seen in Figure 5a. The interaction with the [D]penicilamine residue must have been preferable, as the interaction with the glycine residue ceased after an additional 60 ps but the association with the [D]penicillamine persisted for another 180 ps. The sodium ion that was bound to the C-terminus by the beginning of production also bound to the carbonyl of phenylalanine as seen in the beginning of Figure 5e. Although this joint association did not last long, it reoccurred at 135 ps and persisted for 130 ps. For the duration of the simulation, this ion remained bound to the terminal group only. Relatively free rotation about the bond to the carboxylate group helps to account for the observations of different ions in association with the terminus and backbone groups. While one of the terminal oxygen atoms was bound to the same sodium ion for the entire simulation, the other oxygen atom was free to participate in associations with other ions. It is clear that the interaction between the sodium ion and the oxygen atom was sufficient to overcome repulsion between the sodium ions to allow these arrangements to persist for some time during the trajectory.

Ion binding events were reflected in the radial distribution functions and coordination numbers from the simulation. Radial distribution functions, $g(r)s$, between the peptide and the solvent have been calculated. In order to further characterize the solution

Table III Radial Distribution Functions

	Species	1st Max (nm)	1st Min (nm)	CN	2nd Max	2nd Min	CN
1	NT—H_2O	0.27	0.35	3.7	0.49	0.59	—
2	CT—H_2O	0.37	0.47	9.4	—	—	—
3	C=O—H_2O	0.29	0.41	4.4	—	—	—
4	N—H—H_2O	0.29	0.33	0.91	—	—	—
5	Na^+—OH_2	0.25	0.31	5.6	0.45	—	—
6	Cl—OH_2	0.33	0.39	7.7	0.51	—	—
7	NT—Na^+	—	—	—	—	—	—
8	CT—Na^+	0.27	0.39	1.5	0.47	.63	1.9
9	C=O—Na^+	0.23	0.33	0.25	0.49	—	—
10	N—H—Na^+	0.39	0.45	0.25	—	—	—
11	NT—Cl^-	0.31	0.41	0.45	0.53	0.65	1.2
12	CT—Cl^-	—	—	—	—	—	—
13	C=O—Cl^-	0.39	0.47	0.10	—	—	—
14	N—H—Cl^-	0.35	0.39	0.04	—	—	—
15	Na^+—Na^+	0.37	0.49	0.16	0.63	0.73	0.61
16	Na^+—Cl^-	0.31	0.37	0.04	0.51	0.61	0.82
17	Cl^-—Cl^-	0.53	0.65	0.35	0.77	0.87	1.3
18	Arom—OH_2	0.47	0.61	23.8	0.75	0.91	—
19	SS—OH_2	0.47	0.43	3.43	0.63	0.71	32.7
20	Center of Mass—OH_2	0.31	0.35	—	—	—	—

environment, $g(r)s$ between DPDPE and ions, ions and water, and ions and ions have been calculated as well. Results are summarized in Table III. Coordination numbers, found by integration of the radial distribution function through the first minimum, can also be found in Table III for each well-defined minimum. [Second coordination numbers are found by integrating the $g(r)$ from the first minimum through the second minimum and were only calculated when the second peak in the $g(r)$ was sufficiently well defined.]

Figure 6 displays the radial distribution functions between DPDPE and water. The first peak between the N-terminus and water was slightly lower than that observed in the simulation of DPDPE in pure water, ostensibly due to the partial occupation of potential solvent binding sites by chloride ions during parts of the simulated period. The $g(r)$ between the N-terminus and chloride ion, shown in Figure 7, indicated a well-defined contact interaction with a coordination number of 0.45. This demonstrates that some chloride ion was bound to the N-terminus in about half of the configurations sampled. The well-defined second peak corresponds to a solvent separated interaction. This second peak, integrated to the minimum at 0.65 nm, produced a coordination number of 1.2, illustrating that one chloride ion was, on average, within 0.65 nm of the N-terminus for the entire trajectory.

The effect of ion binding on peptide solvation was even more dramatic for the C-terminus, as shown in Figure 6. A comparison with the radial distribution function between the N-terminus and water shows that the first peak for the C-terminus was lower, indicating fewer bound waters, and it was more diffuse with a less well-defined minimum. This is consistent with the observed binding of sodium ions to the C-terminus. Recall that a sodium ion was bound to an oxygen atom of the terminal group, or between the oxygen atoms, for the entire trajectory. Several instances of additional sodium binding to this group were also observed. It is expected that occupancy by sodium ions would reduce the hydration of this group. Sodium ion occupancy at the C-terminus is supported by the radial distribution function between these species (Figure 7). The first peak is large, with a maximum at 0.27 nm. It integrated to 1.5, indicating that an average of 1.5 sodium ions were in direct contact with the C-terminus over the trajectory. This is consistent with the binding of one sodium ion to the carboxylate group for the duration of the simulation and a second ion present about half of the time, which is confirmed by the distance time histories between sodium ions and the peptide (Figure 4). The second peak in this $g(r)$ displays some unusual structure that could have been due to solvent-mediated interactions or interaction with sodium ions bound to neighboring backbone groups. To elucidate the basis for this structure, configurations of DPDPE, solvent, and ions were investigated. It was determined that the first peak in the

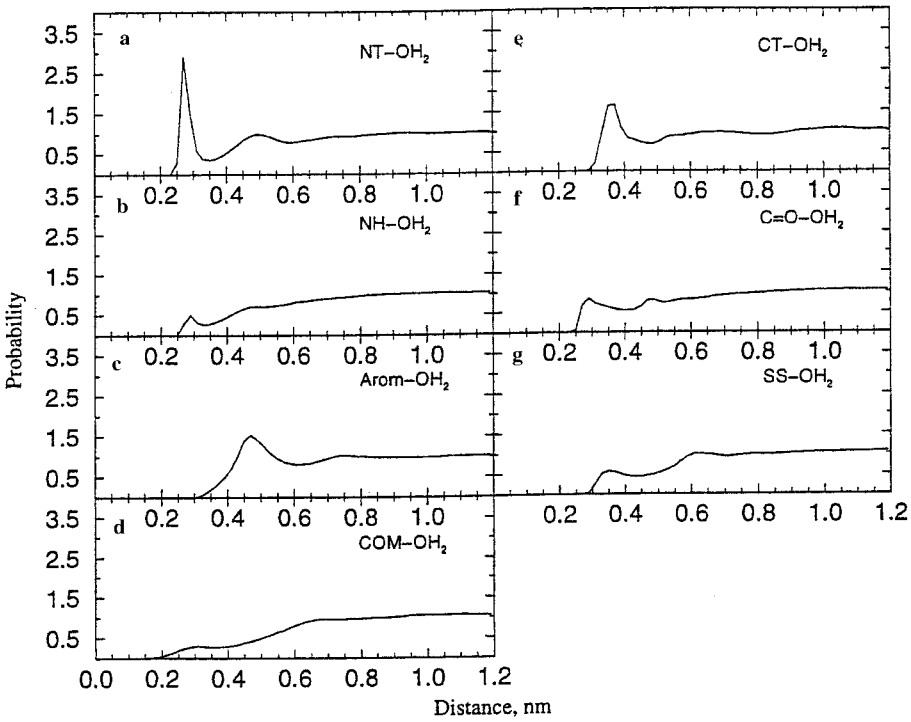

FIGURE 6 Radial distribution functions between DPDPE and H_2O for the DPDPE in NaCl simulation. (a) NT–OH_2, (b) NH–OH_2, (c) Arom–OH_2, (d) COM–OH_2, (e) CT–OH_2, (f) C=O—OH_2, and (g) SS—OH_2.

$g(r)$ corresponds to a sodium ion between the oxygen atoms of the carboxylate group. The first "shoulder" on the second peak, with a maximum at 0.47 nm, corresponds to an arrangement where another sodium ion interacted with both an oxygen atom of the carboxylate group and the carbonyl oxygen of phenylalanine. While water molecules were in the solvation shell of this sodium, the interactions with both of the oxygen atoms on the peptide were contact interactions. The second "shoulder" on this split peak, with a maximum at 0.55 nm, represents interaction of the carboxylate group with a sodium ion bound to the phenylalanine carbonyl, but not to the to the carboxylate group itself. The coordination number corresponding to the second minimum, 1.9, indicates that, on average, nearly two sodium ions were within 0.55 nm of the carboxylate carbon.

Any $g(r)$ will approach unity at large values of r, indicating a return to a bulk distribution of solvent as the reordering effect exerted by the solute diminishes, as seen in Figure 6a and e. In certain systems, however, physical screening due to the size of the solute may require unusually long distances to observe this convergence. This effect can be seen in the radial distribution functions between the peptide backbone and water (Figure 6b and f). Figure 6b is the $g(r)$ between the nitrogen atom of the N—H of the peptide group and water oxygen. Figure 6f is the $g(r)$ between the carbonyl oxygen of the peptide group and water oxygen. The radial distribution function between the N—H group and water was obtained by calculating the $g(r)$ for each of the four N—H groups of the backbone and then averaging over all such groups. The same procedure was used to obtain the $g(r)$ between the backbone carbonyls and water. The $g(r)$ pictured then represents the average interaction between the backbone group and the solvent. The results obtained for these groups are similar to those obtained for DPDPE in pure water. Both types of backbone groups had first peaks with heights less than one, indicating that there were fewer water molecules around these groups, on average, than would be expected for a random distribution of solvent around a single atom. This is a physical screening effect due to steric interactions of the peptide. These groups showed a similar behavior in pure water and the slight differences observed are to be expected due to association of sodium and chloride ions to these backbone groups.

Three additional radial distribution functions are displayed in Figure 6. Pertinent values can be found in Table III. Figure 6c is the $g(r)$ between the aromatic

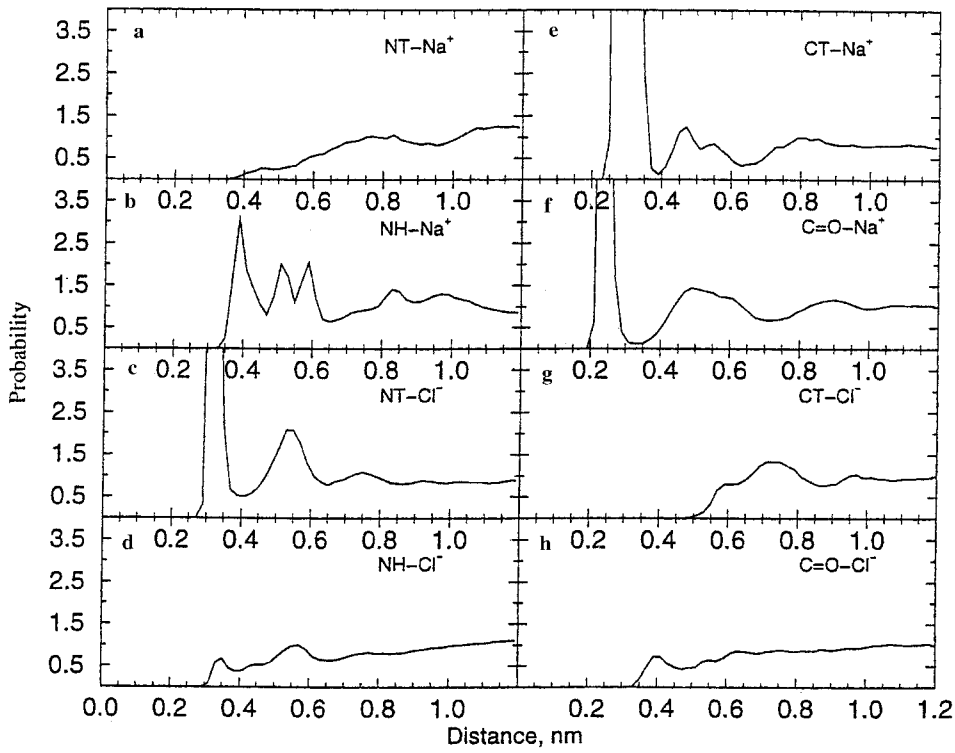

FIGURE 7 Radial distribution functions for terminal and backbone groups of DPDPE to ions for the DPDPE in NaCl simulation. (a) NT–Na^+, (b) NH–Na^+, (c) NT–Cl^-, (d) NH–Cl^-, (e) CT–Na^+, (f) C=O–Na^+, and (g) CT–Cl^-, and (h) C=O–Cl^-.

groups and water. The radial distribution function was calculated for the center of the tyrosine ring to water and for the center of the phenylalanine ring to water. The results were averaged to produce a picture of the general solvation behavior of the aromatic groups. The first solvation shell was broader, with a less well-defined minimum than was observed for terminal groups, but still exhibited definite structure. The coordination number indicates an average of 24 water molecules around these groups. This pattern is expected due to the hydrophobic nature of aromatic groups. It should be noted that these rings extend into solution and may very well experience the least screening from the rest of the peptide of any of the groups considered. In addition, recent studies have shown that hydrophobic groups have defined solvation shells and enhance the hydrogen-bonding network in water, acting like structure makers, forming a clathrate-like structure, as seen in the case of tetraalkylammonium salts.[61–65]

Figure 6g displays the distribution function of the disulfide groups. Its solvation shells were not as well defined as some of the other groups investigated. This can be understood by remembering that sulfur carries a low effective charge in the OPLS force field,[52,57] and the group is undoubtedly subject to physical screening from the peptide. The last $g(r)$ calculated was between the center of mass (COM) of the peptide and water. While it is less straightforward to interpret the radial distribution function between this kind of global peptide group and the surrounding solvent, a kind of general screening of the center of mass of the peptide from solvent was observed. The function never attained a value greater than unity, out to the limit of the accumulation of the histogram, ostensibly indicating that fewer water molecules were found around the peptide, on average, than would be expected for a random distribution of solvent due to physical screening or steric interactions. A radial quantity such as $g(r)$, however, which provides detail on local structure for isotropic systems, must be extended to give general characterization of the more global solvation traits of the system.[66,67]

The radial distribution functions between the backbone N—H groups and chloride ions and between backbone carbonyl groups and sodium ions are presented in Figure 7. The $g(r)$ between the carbonyl groups and sodium ions displays a very well-defined first maximum and minimum. The first coordination number of 0.25 demonstrates that a sodium ion was bound to one of the carbonyl groups in one quarter of the configurations sampled. The second peak contains

contributions from solvent-mediated interactions and the sodium ion that was bound simultaneously to the carbonyl of phenylalanine and the C-terminus. The slight shoulder on the second peak of this $g(r)$ is likely due to the sodium ion attached to the C-terminus but not actually to the carbonyl of the phenylalanine residue. The N—H backbone groups display what may seem like surprising interaction with sodium ions. Because both groups are positively charged, it might be expected that no well-defined maxima or minima would be seen. Through examination of configurations, it was determined that this structure was observed due to the proximity of the N—H groups to the carbonyls, both within the peptide planes and in intramolecular hydrogen bonds, where a sodium ion was often bound. The first peak integrated to a value of 0.25, the same value obtained for carbonyl to sodium, as would be expected if the peak in the N—H to sodium $g(r)$ was actually due to the sodium ion bound to the carbonyl oxygen. The minimum in the N—H to sodium $g(r)$ occurred at 0.45 nm, a larger value than the minimum in the $g(r)$ between the carbonyl groups and sodium and much larger than the contact values of the Lennard–Jones terms in the potential. This is consistent with a probable average distance between the nitrogen of the N—H and a sodium ion bound to the oxygen of an adjacent carbonyl. These features, which occurred at larger distances, reflect sodium ions bound to carbonyl oxygen atoms on different amino acid residues.

Comparison to the solvation of DPDPE in solution with the BHM sodium chloride parameters reveals differences primarily due to observed differences in interaction of ions with the peptide. In the previous simulation, all nine chloride ions bound to the N-terminus, or near it. This so dramatically reduced the solvent in the vicinity that all structure in the N-terminus–water $g(r)$ was lost. At the other extreme, no sodium ion association with DPDPE was observed in that simulation, and therefore the solvation characteristics of the carboxylate group were essentially unchanged from what was observed in pure water. Subsequently, any deviation from solvation currently observed due to sodium ion binding is in contrast to what was observed previously. Direct comparison of the solvation of the peptide backbone when OPLS sodium chloride is present (instead of BHM) is not possible through the interpretation of radial distribution functions. The relatively short trajectories performed with the BHM ions did not furnish enough configurations to obtain adequate statistics for their calculation.

Comparisons, in terms of ion solvation, between the two models are feasible, however. In the current simulation, both the sodium and chloride ions had well-defined first solvation shells, as indicated by the radial distribution functions between the ions and water (Figure 8). Sodium, known as a structure-making ion,[68–71] appeared to have a tighter shell, as would be expected due to its smaller size and higher charge density. Integration of the $g(r)$ up to the first minimum provided a coordination number for sodium of 5.6 (Table III). This is in good agreement with observed experimental values for sodium ion, which indicate octahedral coordination for this ion[71] although recent simulations have questioned this value.[72] The slight deviation from six molecules of water was likely due to binding with the peptide. A sodium ion would have to sacrifice an interaction with a solvent molecule in order to bind to the peptide, reducing its average coordination by water. Chloride also had a well-defined first solvation shell, but the $g(r)$ did not drop to as low a first minimum as the sodium to water $g(r)$. While chloride is not considered to be a structure-breaking ion, its larger radius and lower charge density provide it with less ability to pack water molecules efficiently around itself,[71,73] and it would therefore have a less well-ordered solvation shell. The coordination number for this ion was found to be 7.7, in reasonable agreement with the experimental value of eight.[70,74] Again, the slight deviation from the experimental value could be due to interaction of chloride ions with DPDPE.

Ion solvation properties were also investigated in the DPDPE–salt simulation that employed the BHM model for the ions. There, the first peak in the radial distribution function between sodium ion and water occurred at a slightly smaller distance (0.230 nm). It was also wider, or more diffuse, than in the current simulation. This could be due to the sodium ion's smaller size in the OPLS force field, which leads to a higher charge density and allows the ion to pack water molecules around itself more efficiently, leading to a tighter, better organized shell. The first peak in the radial distribution function between the chloride ion and water occurred at similar distances in both force fields, with the peak for the BHM chloride occurring at a slightly closer distance (0.326 nm), consistent with its smaller size. This peak was also more diffuse for the BHM ion, although not to the same degree as for sodium. This may seem surprising, given that the chloride ion is smaller in the BHM force field than in OPLS. Chloride, however, is not a strong structure-making ion, due to its relatively large size and negative charge, and its solvation shell would not be expected to be as sensitive to small changes in size as that of the sodium ion.

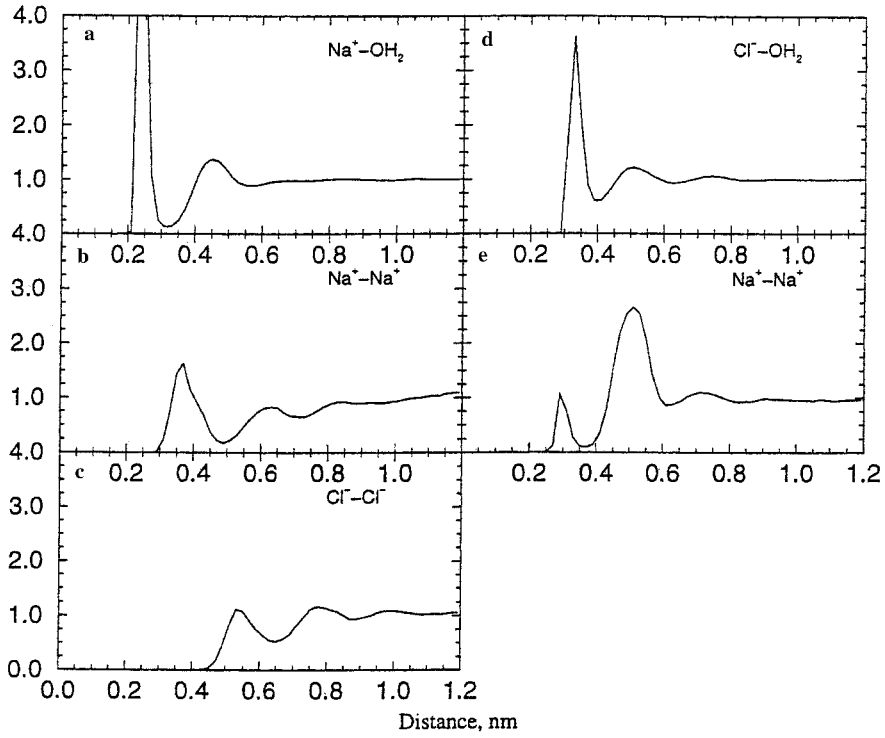

FIGURE 8 Radial distribution functions between ions and between ions and solvent for the DPDPE in NaCl simulation. (a) Na^+–OH_2, (b) Na^+–Na^+, (c) Cl^-–Cl^-, (d) Cl^-–OH_2, (e) Na^+–Na^+.

The solvation properties of the ions in both force fields (when in solution with a peptide solute) can be further investigated by calculating the pair energy distributions for the OPLS ions and comparing the results to those from the previous simulation with BHM ions. These distributions were obtained by calculation of the Coulombic and Lennard–Jones contributions to the potential energy between the ions and the atoms of each water molecule in the system for every configuration. Construction of a histogram of resultant energy values allows the assignment of energies of interaction, or binding energies. The values obtained for the OPLS ions in the current simulation were −93 kJ/mol for sodium and −48 kJ/mol for chloride as compared with pair energies of −101 and −55 kJ/mol, respectively, for the BHM ions in the previous DPDPE–salt simulation. Because the Coulombic charge on the ions is the same in both parameter sets, differences are due to variations in σ and ϵ values and distances between species. Both sodium and chloride bound water more tightly in the BHM force field than in OPLS. Potential consequences will be considered in the last section.

Radial distribution functions between the ions are displayed in Figure 8 as well. The sodium–sodium $g(r)$ indicated a maximum corresponding to an effective interaction that was strongly mediated by solvent. This same type of solvent-stabilized minimum was observed between the chloride ions, although the interaction occurred at a greater distance, as would be expected, due to the larger size of the chloride ion. It may seem unusual that a minimum was observed in the $g(r)$*s* between like ion pairs. In both cases, the interaction was mediated and stabilized by interaction with solvent, and both ions demonstrated a strong interaction with water. It is worth noting that this type of interaction would not be possible if an explicit solvent model were not used.[75] The first peak in the $g(r)$ between sodium and chloride ions integrated to 0.037, indicating that, on average, very few sodium–chloride contact ion pairs were observed, as expected. The height of the second peak in this $g(r)$ indicates that solvent separated interactions between sodium and chloride were preferred. Integration of the second peak provided a coordination number of 0.82, suggesting the existence of a solvent separated sodium–chloride ion pair in about 80% of the configurations sampled. This is in stark contrast to the simulation with BHM ions where no ion pairs, either contact or solvent separated, were observed.

Conformational Properties of DPDPE

The conformational behavior of DPDPE in sodium chloride solution was investigated through the time

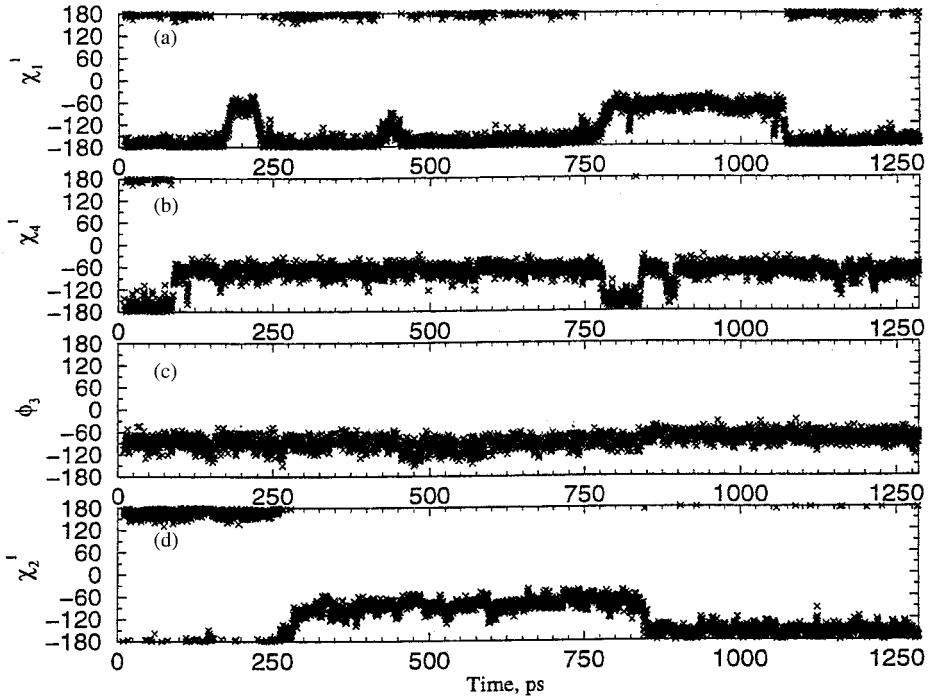

FIGURE 9 Selected dihedral angle time histories for the DPDPE in NaCl simulation. (a) χ_1^1, (b) χ_4^1, (c) ϕ_3, and (d) χ_2^1.

histories of the dihedral angles and through values of the distances associated with the pharmacophore. Many similarities to the behavior of DPDPE in pure water were observed. The most flexible regions of the peptide were, again, the χ_1^1 and χ_4^1 dihedrals associated with the aromatic rings. The time histories for these angles are pictured in Figure 9. The χ_1^1 dihedral, associated with the tyrosine residue, underwent four transitions between the *trans* and *gauche*− well. (Because the freely rotating aromatic side-chain dihedrals exhibit a pattern of three maxima and minima, they can be classified using the three well description of dihedral wells typically associated with alkanes.) There appeared to be a definite preference for the *trans* well, with ca. 73% of the configurations in this conformation, compared with ca. 27% of the conformations in the *gauche*− well. This same preference was observed in the study of DPDPE in pure water. The χ_4^1 dihedral also exhibited marked flexibility with three transitions between the *trans* and *gauche*− wells. Most conformations of this angle occurred in the *gauche*− well, unlike the χ_1^1 dihedral, which demonstrated a preference for the *trans* conformation. Both of these dihedrals made an attempt at another transition during the simulation. The χ_1^1 dihedral attempted a transition from *trans* to *gauche*− at about 425 ps. The energetic barrier to the *gauche*− well was never breached and the angle returned to the *trans* conformation. The χ_4^1 dihedral attempted a transition from its preferred *gauche*− conformation to the *trans* conformation at about 875 ps. Like the attempted transition of χ_1^1, the barrier to the *trans* well was not crossed and the conformation returned to the preferred conformation. (Populations of χ_1^2 and χ_4^2 were not investigated due to the expected ease of sampling of all energetic wells and the subsequent lack of populations in distinct states.)

The backbone of the peptide was relatively rigid, which is consistent with the constrained nature of the macrocycle. As observed in the simulation of DPDPE in water, even ϕ_3 (displayed in Figure 9) and ψ_3, associated with glycine, exhibited little movement over the simulated period and fluctuated about an average value. Glycine dihedrals have a low barrier to rotation due to the lack of a carbon sidechain and have been classified as having one energetic well in accordance with Ramachandran plots for this residue.[10,76,77] It is a bit surprising that more flexibility was not observed. This is especially true, given the flexibility of the dihedrals associated with the disulfide bridge.

The macrocycle of DPDPE is formed through a disulfide linkage or bridge between the sulfur containing sidechains of the two [D]penicillamine residues. Molecular modeling, mechanics, dynamics, and NMR have been used to study motion of this linkage.[40] The

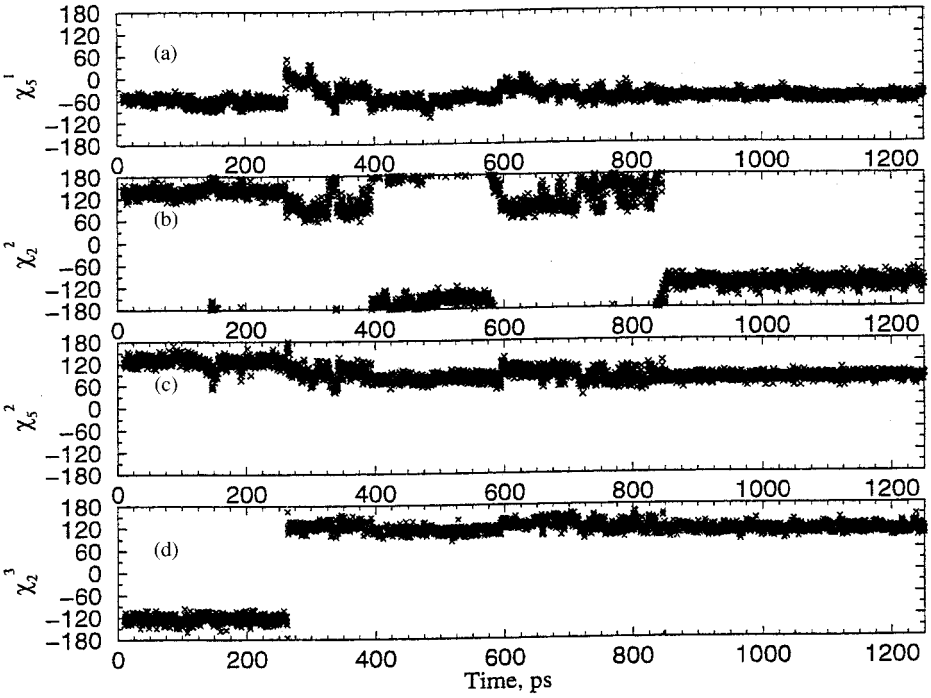

FIGURE 10 Selected dihedral angle time histories for the DPDPE in NaCl simulation. (a) χ_5^1, (b) χ_2^2, (c) χ_5^2, and (d) χ_2^3.

existence of the linkage between the sulfur atoms on [D]penicillamine-2 and [D]penicillaime-5 limits the conformational freedom along the C_α—C_β bond. The dihedral angles associated with the disulfide bond, χ_2^2, χ_2^3, and χ_5^2, are therefore described as having energy minima at $\pm$ 0°, or simply a positive and negative state.[40] Time histories for dihedral angles associated with this linkage are shown in Figures 9 and 10. Transitions were observed between the *trans* and *gauche*− states for the χ_2^1 dihedral. Populations of conformations in the states were quite similar. The χ_2^2 dihedral, also associated with the first [D]penicillamine residue, experienced three transitions between the positive and negative states. While conformations in the states were shared nearly equally, the transition from the positive state to the negative state at about 835 ps appeared to be accompanied by a drop in the potential energy of the solute (Figure 2), which would indicate an energetic preference for this conformation. The χ_5^1 dihedral remained in the energetic well associated with dihedral angle values of less than zero for the entire simulation, except for a very brief transition at 260 ps. It appears that this angle broached the barrier to rotation and made it into the positive well, but was not stable there and quickly returned to the original conformation.

Similarly, the χ_5^2 dihedral of the second [D]penicillamine residue remained in the energetic well associated with dihedral values greater than zero for the entire simulation except for a very brief excursion to the negative well at 260 ps. This was such a brief event that it contributed less than 0.1% to the total conformations. Both of these transient events appear to have occurred in concert with a conformational change of the χ_2^3 dihedral. After sampling conformations in the negative state, this dihedral made a rapid and definitive transition to the positive state at 260 ps. Except for a very brief excursion back to the negative state at 845 ps, the dihedral remained in a conformation in the positive well for the duration of the simulation.[40]

The dihedral angles associated with the disulfide linkage exhibited dramatically enhanced flexibility over that observed for the same dihedrals in the pure water simulation. While this was likely due to the presence of sodium chloride in solution, the transition in the χ_2^3 dihedral, which seemed to precipitate the conformational changes along the disulfide bridge, is difficult to link to ion binding events in time. A sodium ion, bound to the carbonyl oxygen of phenylalanine, did leave this group at about 260 ps (Figure 5e). It is not possible to determine a single causative event, however. It is possible that the sodium ion had stabilized the initial conformation of the disulfide bridge, and its departure led to sufficient destabilization of that conformation, so that a conformational

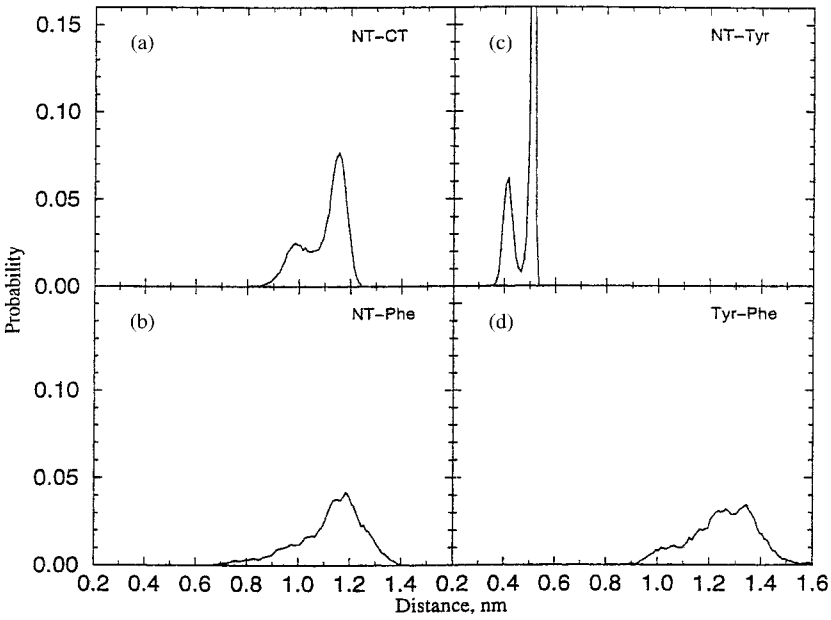

FIGURE 11 Pharmacophore distance probability distributions for the DPDPE in NaCl simulation. (a) NT-CT, (b) NT-Phe, (c) NT-Tyr, and (d) Tyr-Phe.

change was precipitated. This is not certain since, however, since this ion had left this same carbonyl at 140 ps and no transition in the disulfide dihedral angles was observed. On the other hand, the changes in the dihedrals may have instigated the departure of the ion. It is also possible that the effect of sodium chloride on the conformation of the peptide is due to a nonspecific effect that is not directly attributable to ion binding but to more general charge screening effects.

Finally, distances between groups associated with the pharmacophore, or pharmacologically relevant portion, of DPDPE were investigated. This pharmacophore can be characterized by distances between four groups: amino terminus to carboxylate terminus or the end-to-end distance; N-terminus to the center of the tyrosine ring, N-terminus to the center of the phenylalanine ring, and the distance between the centers of the tyrosine and phenylalanine aromatic rings. These four distances were calculated for all configurations of the peptide sampled during the simulation and were used to construct a probability distribution, shown in Figure 11. The slight shoulder in the distribution of distances between the N-terminus and the C-terminus is a reflection of changes in the conformation of the χ_1^1 dihedral angle of the tyrosine residue. The smaller peak corresponds to ca. 27% of the conformations in which χ_1^1 was in the *gauche*− conformation. The overall width of the distribution is a reflection of the wider range of distances expected, given the enhanced flexibility of the peptide in sodium chloride solution. The distribution of distances between the N-terminus and tyrosine is very similar to what was observed in the simulation of DPDPE in pure water. Probability distributions involving the phenylalanine residue are also very similar to those observed in the pure water simulation, except that their distributions are slightly wider, which reflects the improved flexibility of the peptide.

The conformational behavior of DPDPE in this simulation has been compared to experimental structural data. As previously stated, DPDPE has been studied by a variety of experimental techniques including x-ray crystallography and NMR. While the focus of our studies of DPDPE has been the elucidation of processes underlying the Hofmeister series through an examination of the correlation between solvent and cosolvent behavior with the peptide, comparison to experimental data provides a vehicle for ensuring that the computational models and methods used are rooted in natural phenomena and adds confidence to predictions arising from their use.

Comparison has been made between the structure of DPDPE in the current molecular dynamics simulation and the x-ray crystallographic structure of DPDPE[44] through the calculation of root mean square (rms) displacements for the C_α atoms of the peptide backbone. These values represent the similarity (or difference) between the arrangement of C_α atoms of the peptide in the molecular dynamics simulation, as compared with the arrangement of C_α atoms in the experimental x-ray crystallographic structure. Identi-

cal arrangements of C_α atoms would result from identical backbone conformations and would produce a rms value of 0 Å. Deviation between the structures compared increases as the value of rms increases. Values of rms fluctuate over a simulated period as the conformation of the peptide changes. Our comparison focused on the C_α backbone due to the conformational freedom of the aromatic sidechains.

Five representative structures from the simulation trajectory were chosen for comparison to the x-ray structure, corresponding to conformers of the peptide at 0.20, 0.40, 0.60, 0.80, and 1.00 ns. Values obtained were, respectively, 0.96, 0.78, 0.61, 0.92, and 0.84 Å. These values indicate good agreement with (or little deviation from) the C_α arrangement observed in the crystal structure. The largest value of 0.96 Å is within the resolution of the crystal structure itself.[44] Fluctuations in the value of the rms displacement occurred in conjunction with conformational changes in the backbone over the simulated period. Notice that the value did not progressively increase (or decrease) during the simulation, which would correspond to a gradual departure from (or convergence to) a conformation similar to the x-ray structure. Instead, the rms values fluctuated about a small value, which is consistent with a system sampling conformational space under conditions of equilibrium. It is worth noting that the C_α backbone arrangement in the current simulation is in better agreement with the crystal structure than that observed in the previous simulation of DPDPE in aqueous sodium chloride solution. This lends confidence to the use of OPLS parameters when ions are included in simulation studies of peptides in aqueous solution.

CONCLUSIONS

A molecular dynamics simulation of DPDPE in aqueous solution of OPLS sodium chloride has been performed. Extensive binding of both sodium ions and chloride ions to the terminal groups and backbone of the peptide was observed. Variation in the duration of binding events existed, ranging from 2 to 1285 ps. Chloride ions appeared to be more likely to be exchanged after binding than did sodium ions. Several instances of repeated ion binding occurred, with the same ion binding repeatedly to the same group on the peptide or to neighboring groups. In some cases, an ion was shared, thus binding simultaneously to adjacent groups on the peptide. This behavior is substantially different from the binding interactions observed when DPDPE was simulated in an aqueous solution of Born–Huggins–Mayer sodium chloride. In that simulation, all chloride ions bound to the peptide. It should be noted, however, that the entire trajectory in the previous simulation was only 200 ps long. Some of the chloride ion binding events observed in the current simulation were nearly that long, or longer; however, the equilibrium constant in the present simulation for chloride binding to the amino terminus is greatly reduced using the OPLS parameters. Clearly, the differences in values of σ and ϵ in the two force fields changed the binding, regardless of the length of the trajectory. Differences were also observed in the interaction of sodium ions with DPDPE. While substantial binding of sodium ions occurred in the current simulation, no sodium ions were observed to interact with the peptide when BHM sodium parameters were used. In fact, the average distance between sodium ions and the peptide increased in that simulation, and the ions were observed to move away from DPDPE to form an outer sphere complex.

Variation in the interactions of the ions from the two force fields with DPDPE was also reflected in the solvation properties of the ions. There was a greater difference in the radial distribution functions and pair energies of the two sodium models, and there was a greater difference in the behavior of the sodium ions in the two force fields with DPDPE. Pair energy distributions helped elucidate these observations. These distributions indicated that both sodium and chloride ions bound water less tightly in the OPLS force field than in the BHM. This may explain the difference in binding with the peptide. In order for an ion to engage in a contact interaction with the peptide, it must lose at least one of its waters of solvation. Due to their higher binding energy, BHM sodium ions were less likely to undergo desolvation and therefore less likely to interact directly with DPDPE. This may also explain, at least in part, the absence of any contact or even solvent separated sodium-chloride ion pairs in the previous simulation. One of the ions must lose a water molecule from its solvation shell to participate in a solvent separated ion pair, and both ions must undergo desolvation to engage in a contact pair.

The χ_1^1 and χ_1^4 dihedrals were the most flexible regions of the peptide, which is consistent with the constraining effect exerted by the macrocycle. The dihedrals associated with the disulfide bridge exhibited increased flexibility over that observed for DPDPE in pure water. While this conformational flexibility is likely due to the effect of the salt, the precise nature of that effect is not clear. The data suggest that binding events and conformational changes are correlated in time, but whether the release of a bound ion precipitated the conformational change or the confor-

mational change precipitated the departure of a bound ion from the peptide is not clear. It is also possible that ion binding may exert a nonspecific effect on the conformational preferences and stability of the peptide. Yet again, the effect may be direct but delayed in time. Pharmacologically, the aromatic groups on DPDPE are associated with the pharmacophore and are believed to be central to its affinity for the δ-opioid receptor. The conformation of the rings in the bound form is thought to be determined by the structure of the receptor itself.[20,38,39] From the point of view of drug design, a structure with less flexibility is desired because a reduced entropy cost upon binding of the ligand to the receptor should enhance binding affinity. This suggests that restraining the χ_1^1 dihedral, and especially the χ_4^1 dihedral, may be a potential target for design of peptide opiate agonists, presuming the dihedral is constrained in a pharmacologically active conformation.[20,78–80]

This simulation was primarily undertaken to further the characterization of the solvent environment around a peptide, such as DPDPE, in the presence of a salt, such as sodium chloride. Observations will contribute to the elucidation of the Hofmeister series. In order for those contributions to be useful, observations must be carefully acquired and cautiously interpreted. To this end, it is important to have longer simulations, with more configurations and subsequently improved statistics. This, in turn, allows for further characterization of the solvent environment around the peptide and how that environment changes when ions are introduced, which is necessary if these effect are to be investigated. Care must be exercised when choosing parameters for ions. As demonstrated here, sensitivity to ion parameters used does seem to exist. Parameters and model potentials are constantly being developed and improved and one can hope that accuracy of results obtained in molecular dynamics simulations will continue to improve accordingly.

REFERENCES

1. von Hippel, P.; Schleich, T. Acc Chem Res 1969a, 2, 257.
2. von Hippel, P.; Schleich, T. Biological Macromolecules, Vol. 2; Timasheff, S. N., Fastman, G. D., Eds.; New York: Marcel Dekker, 1969; p 417.
3. Robinson, D. R.; Jencks, W. P. J Am Chem Soc 1965, 87, 2470.
4. Nandi, P. K.; Robinson, D. R. J Am Chem Soc 1972, 94, 1299.
5. Nandi, P. K.; Robinson, D. R. J Am Chem Soc 1972, 94, 1308.
6. Franks, F.; Eagland, D. CRC Crit Rev Biochem 1975, 3, 165.
7. Flanagan, M. A.; Ackers, G. K.; Matthew, J. B.; Hanania, G. I. H.; Gurd, F. R. N. Biochemistry 1981, 20, 7439–7449.
8. Perkyns, J. S.; Pettitt, B. M. J Phys Chem 1995, 99, 1.
9. Giese, A. C. Cell Physiology; Philadelphia: W. B. Saunders, 1973.
10. Stryer, L. Biochemistry; New York: W. H. Freeman, 1997.
11. Tanford, C. Adv Protein Chem 1970, 24, 1.
12. Wood, R.; Wicker, R.; Kreis, R. J Phys Chem 1971, 75, 2313.
13. Collins, D. D.;. Washabaugh, M. L. Quart Rev Boiphys 1985; 18, 323–422.
14. Shih, Y. C.; Prausnitz, J. M.; Blanch, H. W. Biotech Bioeng 1992, 40, 1155.
15. Timasheff, S. N. Biochemistry 1992, 31, 9857.
16. De Young, L. R.; Fink, A. L.; Dill, K. A. Acc Chem Res 1993, 26, 614.
17. Coen, C. J.; Blanch, H. W.; Prausnitz, J. M. AIChE J 1995, 41, 996.
18. Perkyns, J. S.; Wang, Y.; Pettitt, B. M. J Am Chem Soc 1996, 118, 1164.
19. Cacace, M. G.; Landau, E. M.; Ramsden, J. J. Quarterly Reviews of Biophysics 1997, 30, 241.
20. Hruby, V. J.; Pettitt, B. M. In Computer Aided Drug Design: Methods and Applications; Perun, T. J.; Propst, C. L., Eds.; New York: Marcel Dekker, 1989; p 405.
21. Rasaiah, J. C.; Friedman, H. L. J Chem Phys 1968, 48, 2742.
22. Bockris, J. O. M.; Reddy, A. K. N. Modern Electrochemistry, Vol. 1, New York: Plenum Press, 1970.
23. Rasaiah, J. C. J Chem Phys 1972, 56, 3071.
24. Hofmeister, F. Arch Exp Pathol Phar 1888, 24, 247–260.
25. Lewith, S. Arch Exp Pathol Pharmakol 1888, 24, 1.
26. Rossky, P. J.; Karplus, M. J Am Chem Soc 1979, 101, 1913.
27. Dang, L. X.; Kollman, P. J Am Chem Soc 1990, 112, 503.
28. Avbelj, F.; Moult, J.; Kitson, D. H.; James, M. N. G.; Hagler, A. T. Biochemistry 1990, 29, 8658.
29. Berendsen, H. J. C., van Gunsteren, W. F.; Zwinderman, H. R. J.; Guertsen, R. G. Ann NY Acad Sci 1986, 482, 269.
30. Smith, P. E.; Pettitt, B. M. J Am Chem Soc 1991, 113, 6029.
31. Smith, P. E.; Pettitt, B. M. J Chem Phys 1991, 95, 8430.
32. Smith, P. E., Marlow, G. E.; Pettitt, B. M. J Am Chem Soc 1993, 115, 7493.
33. Mosberg, H. I.; Hurst, R.; Hruby, V. J.; Galligan, J. J.; Burks, T. F.; Gee, K.; Yamamura, H. I. Biochem Biophys Res Commun 1982, 106, 506.
34. Mosberg, H. I.; Hurst, R.; Hruby, V. J.; Yamamura, H. I.; Galligan, J. J.; Burks, T. F. Proc Natl Acad Sci USA 1983, 80, 5871.

35. Schiller, P. W. The Peptides: Analysis, Synthesis, Biology. Vol. 6: Opioid Peptides: Biology, Chemistry, and Genetics; Udenfriend, S., Meienhofer, J. Eds.; New York: Academic Press, 1984; p 219.
36. Hruby, V. J.; Krstenansky, J. L.; Cody, W. L. Ann Rep Med Chem 1984, 19, 303–312.
37. Aubry, A.; Birlirakis, N.; Sakarellos-Daitsiotis, M.; Sakarellos, C.; Marraud, M. Biopolymers 1989, 28, 27–40.
38. Mierke, D. F.; Said-Nejad, O. E.; Schiller, P. W.; Goodman, M. Biopolymers 1990, 29, 179.
39. Hruby, V. J. Opioid Peptides: Medicinal Chemistry; Rapaka, R. S., Barnett, G., Hawks, R. L., Eds.; Rockville: NIDA Research Monograph 69, 1986; p 128.
40. Hruby, V. J.; Kao, L.; Pettitt, B. M.; Karplus, M. J Am Chem Soc 1988, 110, 3351–3359.
41. Smith, P. E.; Dang, L. X.; Pettitt, B. M. J Am Chem Soc 1991, 113, 67.
42. Mosberg, H. I.; Sobczyk-Kojiro, K. P. S.; Crippen, G. M.; Ramalingam, K.; Woodward, R. W. J Am Chem Soc 1990, 112, 822.
43. Nikiforovich, G. V.; Prakash, O.; Gehrig, C. A.; Hruby, V. J. Int J Pept Protein Res 1993, 41, 347.
44. Flippen-Anderson, J. L.; Hruby, V. J.; Collins, N.; George, C.; Cudney, B. J Am Chem Soc 1994, 116, 7523.
45. Froimowitz, M.; Hruby, V. J. Int J Peptide Protein Res 1989, 34, 88.
46. Froimowitz, M. Biopolymers 1990, 30, 1011–1025.
47. Nikiforovich, G. V.; Balodis, J.; M. D. S.; Golbraikh, A. A. Int J Pept Protein Res 1990, 36, 67.
48. Wilkes, B. C.; Schiller, P. W. J Comput-Aided Mol Des 1991, 5, 293.
49. Chew, C.; Villar, H. O.; Loew, G. H. Biopolymers 1993, 33, 647.
50. Pettitt, B. M.; Matsunaga, T.; Al-Obeidi, F.; Gehrig, C.; Hruby, V. J.; Karplus, M. Biophys J 1991, 60, 1540.
51. Smith, P. E.; Marlow, G. E.; Pettitt, B. M. J Am Chem Soc 1993, 115, 7493.
52. Jorgensen, W. L.; Tirado-Rives, J. J Am Chem Soc 1988, 110, 1657.
53. Brooks, B. R.; Bruccoleri, R. E.; Olafson, B. D.; States, D. J.; Swaminathan, S.; Karplus, M. J Comput Chem 1983, 4, 187.
54. Pettitt, B. M.; Rossky, P. J. J Chem Phys 1986, 84, 5836.
55. Huggins, M. L.; Mayer, J. E. J Chem Phys Eds.; 1933, 1, 643.
56. Tosi, M. P.; Fumi, F. G. J Phys Chem Solids 1964, 25, 45.
57. Jorgensen, W. L.; Gao J. J Phys Chem 1986, 90, 2174.
58. Dang, L. X.; Pettitt B. M. J Phys Chem 1987, 91, 3349.
59. Ewald, P. Ann Physik 1921, 64, 253–287.
60. De Leeuw, S. W.; Perram, J. W.; Smith, E. R. Proc R Soc Lond A 1980, 373, 27–56.
61. Wallqvist, A. Chem Phys Lett 1991, 182, 237.
62. Grunwald, E.; Steel, C. J Am Chem Soc 1995, 117, 5687.
63. Slasher, J. T.; Cummings, P. T. J Phys Chem B 1997, 101, 3818.
64. Garde, S.; Hummer, G.; Paulaitis, M. E. J Chem Phys 1998, 108, 1552.
65. Smith, P. E. J Phys Chem B 1999, 103, 525.
66. Lounnas, V.; Pettitt, B. M.; Phillips, G. N. Biophysical J, 1994, 66, 601.
67. Makarov, V. A.; Andrews B. A.; Pettitt, B. M. Biophysical J 1998, 74, 413.
68. Frank, H. S.; Evans, M. J Chem Phys 1945, 13, 507.
69. Gurney, R. W. Ionic Processes in Solution; New York: McGraw-Hill, 1953.
70. Enderby, J. E.; Neilson, G. W. Rep Prog Phys 1981, 44, 593.
71. Madden, P. A.; Impey, R. W. Ann NY Acad Sci 1986, 482, 91.
72. Rempe, S. B.; Pratt, L. R. J Chem Phys 2001 (in press).
73. Washabaugh, M. W.; Collins, K. D. J Biol Chem 1986, 261, 12477.
74. Enderby, J. E. Ann Rev Phys Chem 1983, 34, 155.
75. Dang, L. X.; Pettitt B. M. J Phys Chem 1990, 94, 4303.
76. Ramachandran, G. N.; Sasisekharan Adv Pro Chem 1968, 23, 283.
77. Richardson, J. S.; Richardson, D. C. The Prediction of Protein Structure and the Principles of Protein Conformation; Fasman, G. D., Ed.; New York: Plenum Press, 1989.
78. Burgess, K.; Ho, K. K.; Pettitt, B. M. J Am Chem Soc 1994, 116, 799.
79. Burgess, K.; Ho, K. K.; Pettitt, B. M. J Am Chem Soc 1995, 117, 54.
80. Qian, X. H.; Shenderovich, M. D.; Kover, K. E.; Davis, P.; Horvath, R.; Zalewska, T.; Yamamura, H. I.; Porreca, F.; Hruby, V. J. J Am Chem Soc 1996, 118, 7280.